AD 297 459

63-2-5

STUDIES OF PLASMA OSCILLATIONS

AEC CONTRACT AT(04-3)-326

(Project Agreement No. 1)

Quarterly Status Report No. 12

1 September - 30 November 1962

M. L. Report No. 999

January 1963

Microwave Laboratory
W. W. Hansen Laboratories of Physics
Stanford University
Stanford, California

STAFF

Contract AT(04-3)-326, Project Agreement No. 1
(Modification No. 2)

1 September - 30 November 1962

FACULTY

G. S. Kino, part time

C. F. Quate, part time

RESEARCH ASSOCIATES

F. W. Crawford, part time

I. L. Freeston, part time

S. A. Self, part time

PROJECT ENGINEER

H. J. Landsbergen, part time

RESEARCH ASSISTANTS

A. B. Cannara, part time

J. F. Knutson, part time

T. W. Sigmon, part time

TABLE OF CONTENTS

LIST OF FIGURES

I. INTRODUCTION

This is the Twelfth Quarterly Report, and covers the period from 1 September to 30 November 1962. This program consists of a study of plasma oscillations with the objective of determining and explaining the mechanism for the growth of instabilities and oscillations in a gaseous discharge, with particular emphasis on the action of sheaths and wave interactions with particles in the discharge. The effect of parameters such as geometric shapes and boundaries, magnetic field, pressure and velocity distributions will be taken into account.

The responsible investigator for this contract is Professor Marvin Chodorow.

II. OBJECTIVE

Close examination of supposedly quiescent plasma generally shows the presence of fluctuations in discharge parameters such as anode voltage, current, number density, light output, etc. These may be coherent or incoherent and usually have strong components in either or both of the frequency ranges, zero to a few Mc/s, and the microwave band. The amplitudes may be quite substantial. For example, anode voltage fluctuations from millivolts to volts are commonly observed in discharges at a pressure of about 1 μ with which we are concerned. The objectives of this program are, then, threefold: (1) to observe the characteristics of these fluctuations (which we shall term "noise"); (2) to determine their generation mechanisms; and (3) to suppress them as far as possible.

Previous reports have dealt with observations of some of the noise characteristics, and suggestions for the generation mechanisms. Some success in suppression has already been achieved by the use of grids and magnetic fields. In this report, further experiments are described, generally designed to elucidate specific points which have arisen from our previous work.

III. THEORETICAL WORK

A. DIPOLE RESONANCE

Previous quarterly status reports[1-3] have dealt with a high-frequency dipole resonance technique for measurement of dc and low frequency components of plasma electron density, and some theoretical work has already been carried out for the case of a cylindrical plasma, taking geometrical factors and a radial variation of number density into account.[4] During the quarter, solutions have been derived by the same variational method for the cases of spherical and infinite plane geometry.[5] The basic results for the resonant frequencies are as follows.

1. Plane Geometry:

$$\omega_0^2 = \frac{\overline{\omega_p^2}}{1 + \gamma_1} \tag{1}$$

$$\gamma_1 = \frac{a}{(c - b) + \left(\frac{b - a}{\epsilon_1}\right)} . \tag{2}$$

Here, $\overline{\omega_p^2}$ corresponds to the mean electron density across the section.

2. Cylindrical Geometry:

For the component varying as $\phi_a (r/a)^n \cos n\theta$, we have

$$\omega_0^2 = \frac{\omega_{p0}^2 \left(1 - \frac{\alpha p}{p + 2}\right)}{1 + \gamma} \tag{3}$$

$$\gamma = \frac{\epsilon_1}{\mu} \left[\frac{1 - \mu \left(\frac{1 - K}{1 + K}\right) \left(\frac{a}{b}\right)^p}{1 + \left(\frac{1 - K}{\mu + K}\right) \left(\frac{a}{b}\right)^p} \right] \tag{4}$$

$$K = 1/\epsilon_1 \left[\frac{1 + \mu(b/c)^p}{1 - (b/c)^p} \right] \tag{5}$$

$$\mu = 1 \ , \ p = 2n \ . \tag{6}$$

3. Spherical Geometry:

For the component varying as $\phi_a\,(r/a)^n\,P_n^m\,(\cos\theta)\cos m\lambda$, ω_0^2 is given by Eqs. (3), (4) and (5), but with

$$\mu = \frac{n}{n+1} \quad , \quad p = 2n + 1 \quad , \tag{7}$$

where dimensions are as given in Figs. 1 and 2, and α is the parameter in the assumed parabolic variation of number density

$$\omega_p^2 = \omega_{p0}^2 \left(1 - \alpha \frac{r^2}{a^2}\right) \quad . \tag{8}$$

We note that for dipole resonance of a plasma in free space, these simplify to $\omega_p^2/\sqrt{1}$, $\omega_p^2/\sqrt{2}$, $\omega_p^2/\sqrt{3}$, respectively.

Although we have not carried out measurements with hollow plasmas, experiments have shown that the resonances become double-humped in this geometry.[6] Since the variational method can be extended to cover the case, this analysis has been carried through and is to be found in Microwave Laboratory Report No. 979.[7] Results are given for symmetrical hollow cylindrical and spherical plasmas, taking into account electrode geometry, the discharge tube walls, and an arbitrary number density distribution.

B. PLASMA IMPEDANCE

Our work on plasma impedance in the frequency range zero to a few Mc/s has suggested that important information on the basic discharge processes and noise mechanisms can be deduced.[8,9] The preliminary theory based on single-stage ionization processes gave an equivalent circuit which did not contain all the terms of the experimentally-determined one. Since two-stage processes are likely to be important in low-pressure mercury-vapor discharges,[10] we are attempting to extend the analysis to include them. This work is at a preliminary stage, and will be reported more fully later.

C. NOISE AND PROBE MEASUREMENTS

About 18 months ago we drew attention to the fact that substantial errors might be made in probe measurements taken in the presence of noise.[3] At that time,

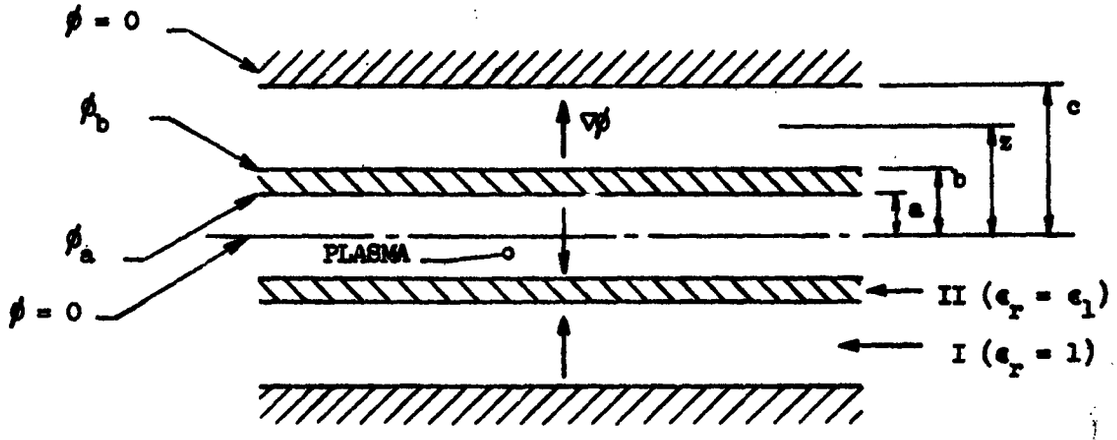

FIG. 1--Plane geometry.

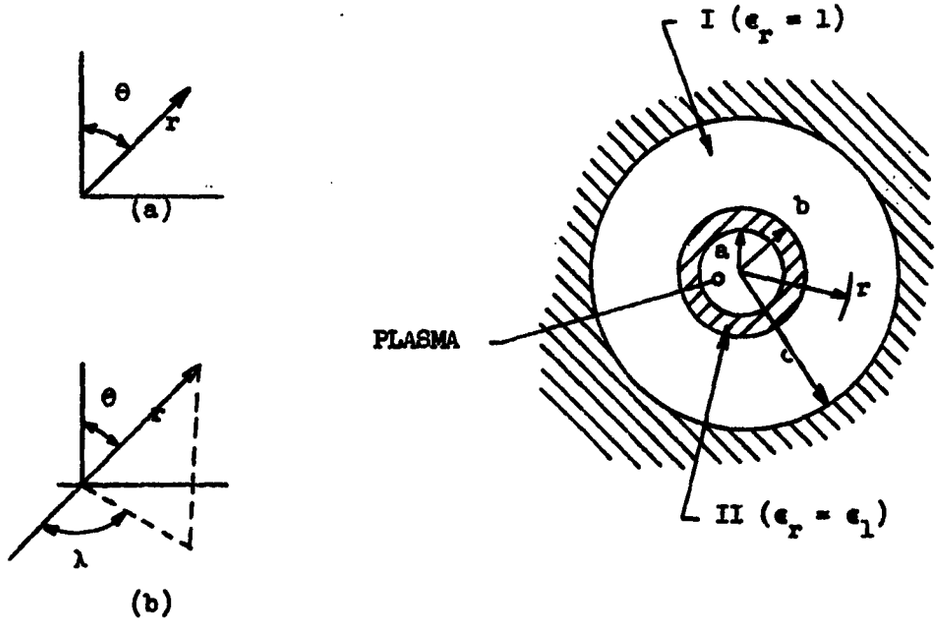

FIG. 2--Cylindrical and Spherical Geometry.
(a) Coordinates for cylindrical system.
(b) Coordinates for spherical system.

it was found that a paper by Garscadden and Emeleus was in press,[11] so our work was temporarily suspended, to avoid duplication. This publication dealt separately with variations in the parameters n_e, V_e and V_s in the expression for the electronic component, i_e, of probe current

$$i_e = k\, n_e \sqrt{V_e}\, \exp\left[\frac{V - V_s}{V_e}\right] , \qquad (9)$$

where k is a constant, V is the probe potential, V_s is space potential and V_e is the electron temperature measured in the same units as V and V_s. The general conclusions were that fluctuations in n_e had no effect, and that fluctuations in V_s or V_e could produce an increase in the dc probe current. If only V_s fluctuates, then the section of the probe characteristic below saturation is translated vertically on the usual $\log i_e/V$ plot so that temperature can still be obtained accurately, though space potential becomes difficult to estimate. Some experiments were described for an effective variation in space potential, and agreement with the theory was obtained.

We have generalized this theory to include simultaneous changes in all three variables, and an arbitrary probe characteristic. The saturation regions have also been studied. This analysis is given in Microwave Laboratory Report No. 980.[12] The basic results are as follows.

For a generalized probe characteristic,

$$i_e = f(n_e, V_s, V_e) , \qquad (10)$$

subject to fluctuations $i_e(t)$, $V_s(t)$, $V_e(t)$, by Taylor's Theorem, we have for the probe current averaged over time t, the expression

$$\frac{\overline{i_e}}{i_e} = 1 + 1/2 \left\{ A_n\, \overline{n_e}(t)^2 + A_s\, \overline{V_s}(t)^2 + A_e\, \overline{V_e}(t)^2 \right\}$$

$$+ A_{ns}\, \overline{n_e(t)\, V_s(t)} + A_{se}\, \overline{V_s(t)\, V_e(t)} + A_{en}\, \overline{V_e(t)\, n_e(t)} , \qquad (11)$$

where $\overline{n_e(t)}$, $\overline{V_s(t)}$ and $\overline{V_e(t)}$ are rms values. The cross-products will disappear if the signals are uncorrelated. The experiments to be described later suggest that the temperature terms are negligible compared with the others so that Eq. (11) simplifies to

$$\frac{\overline{i_e}}{i_e} = 1 + 1/2 \left\{ A_n \overline{n_e(t)}^2 + A_s \overline{V_s(t)}^2 \right\} + A_{ns} \overline{n_e(t)\, V_s(t)} \qquad (12)$$

For the probe characteristic of Eq. (9), and taking correlation of the $n_e(t)$ and $V_s(t)$ fluctuations into account, we arrive at

$$\frac{\overline{i_e}}{i_e} = 1 + 1/2 \frac{\overline{V_s(t)}^2}{V_e} - \sum_1^\infty \bar{c}_n \bar{a}_n \cos \lambda_n \quad , \qquad (13)$$

where $\bar{c}_n$, $\bar{a}_n$ are rms values of the Fourier components of $\left(\frac{V_s(t)}{V_e}\right)$ and $\left(\frac{n_e(t)}{n_e}\right)$, and λ_n is the phase angle between them.

A large-signal analysis is possible if we ignore $V_e(t)$ and assume a single-frequency signal for $V_s(t)$ and $n_e(t)$. We then have

$$\frac{\overline{i_e}}{i_e} = I_0 \left(\frac{V_{sl}}{V_e}\right) + \left(\frac{n_{el}}{n_e}\right) I_1 \left(\frac{V_{sl}}{V_e}\right) \cos \lambda \quad , \qquad (14)$$

where I_0 and I_1 are modified Bessel Functions. The theory of Garscadden and Emeleus does not predict the cross-modulation term since the variables were treated separately.

IV. EXPERIMENTAL WORK

A. NOISE AND PROBE MEASUREMENTS

The analysis just described was verified by modulating the probe potential and discharge current with single-frequency and noise signals. A single-frequency signal in series with the probe simulates a variation in space potential. There should be an increase in probe current corresponding to the first term of Eq. (14). Figures 4a and b indicate close agreement between theory and experiment. The circuits used were as shown in Fig. 3.

Next, simultaneous variation of number density and space potential were made, with varying phase shift between the two signals. This gave the results shown in Fig. 5, and good agreement was obtained between the results and Eq. (14). This confirms, incidentally, that the temperature fluctuations were negligible.

Equation (11) indicates that for uncorrelated signals the noise power is important, and that the noise could be replaced effectively by a single-frequency signal of the same rms value. This was confirmed in experiments where the probe was modulated by a noise signal. Typical results are shown in Fig. 6. It is clear that the approximate equivalence is good up to about the electron temperature.

In practice, the effect of fluctuations is to reduce the current at which the break-point in the probe characteristic occurs. This is clearly visible on Fig. 4b, and will lead to underestimation of the electron density. For example, with a single-frequency noise signal of ΔV volts peak-to-peak, the electron number density will be exp $(\Delta V/V_e)$ times that measured from the experimental break-point, even under ideal conditions. If $\Delta V/V_e$ is not small compared to unity, substantial errors will arise. Further considerations along these lines are given in the report,[12] together with suggestions for an ac method of temperature measurement based on the large-signal theory.

This phase of the work is now considered as completed.

B. ION WAVES

The past quarter has been devoted largely to closer examination of the nature of the radial ion waves proposed to explain the peaks in the low-frequency noise spectrum. In particular, the appropriate boundary condition for an ion wave at

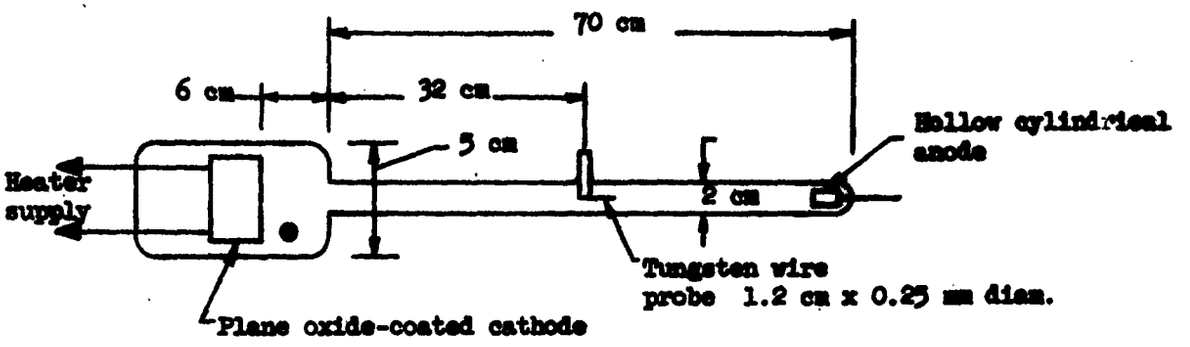

(a) Experimental discharge tube.

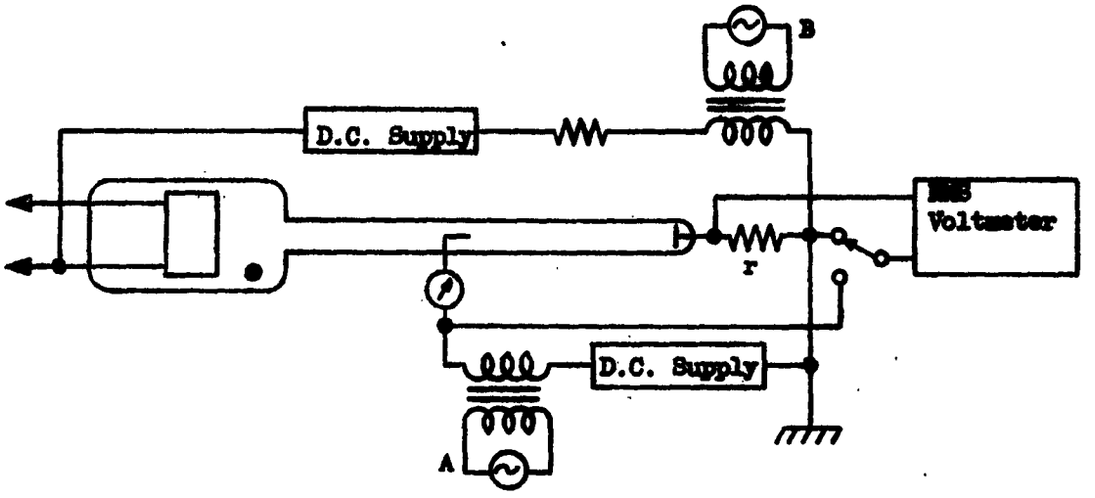

(b) Independent voltage or current injection.

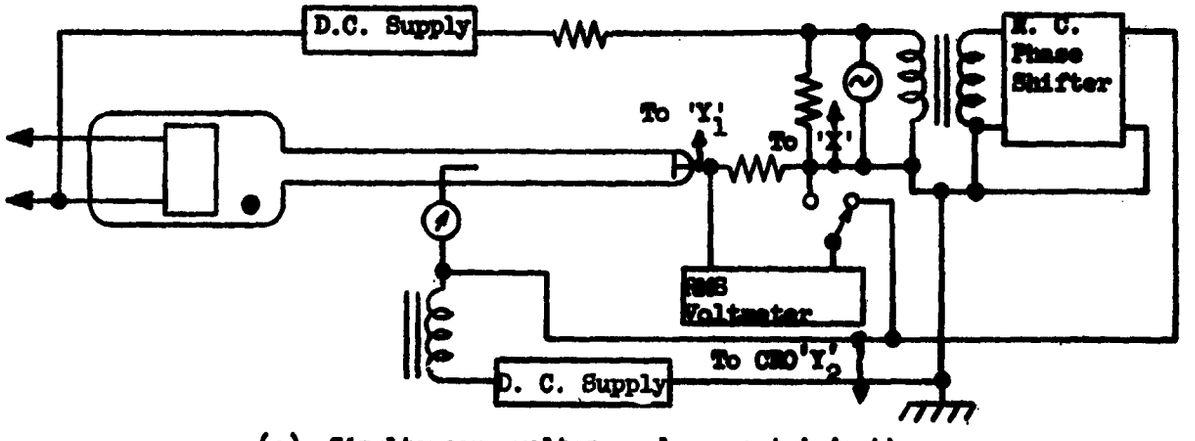

(c) Simultaneous voltage and current injection.

FIG. 3--Experimental discharge tube and circuits.

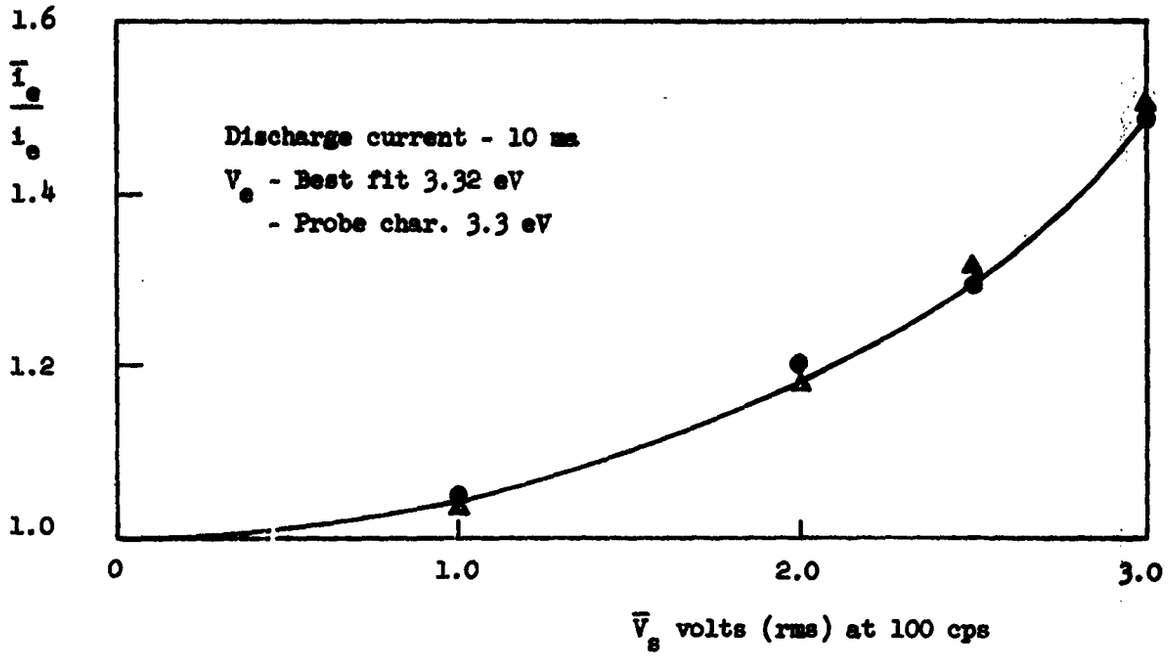

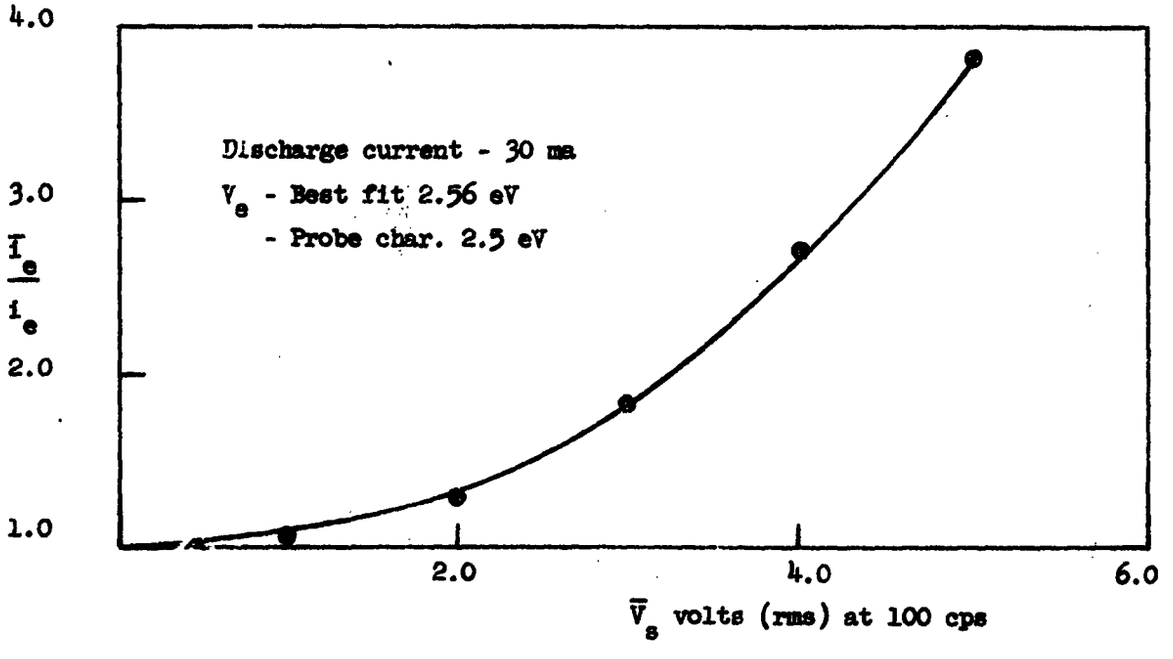

FIG. 4(a)--Probe current increases due to an ac signal in series with the probe.

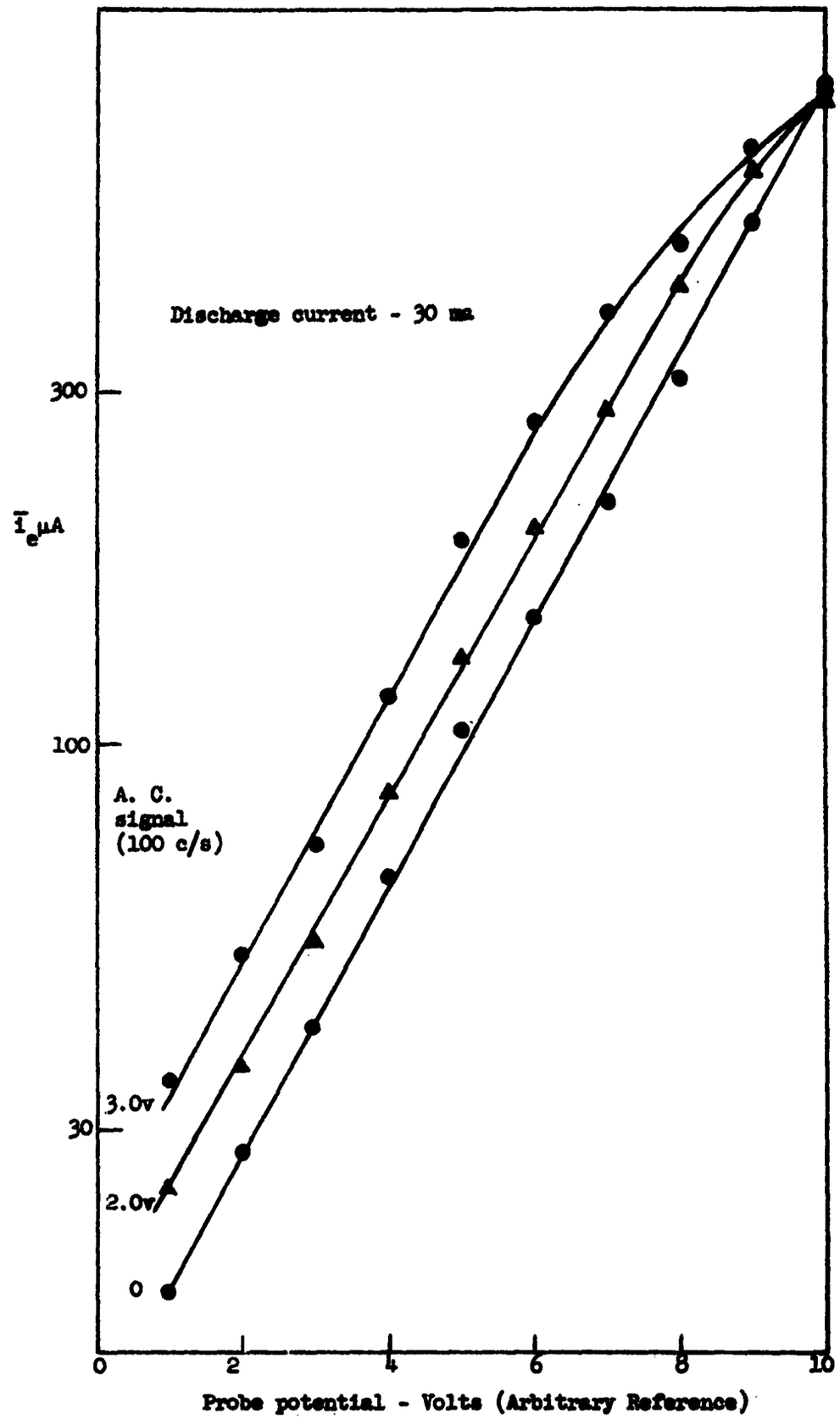

FIG. 4(b)--Probe current increase due to an ac signal in series with the probe.

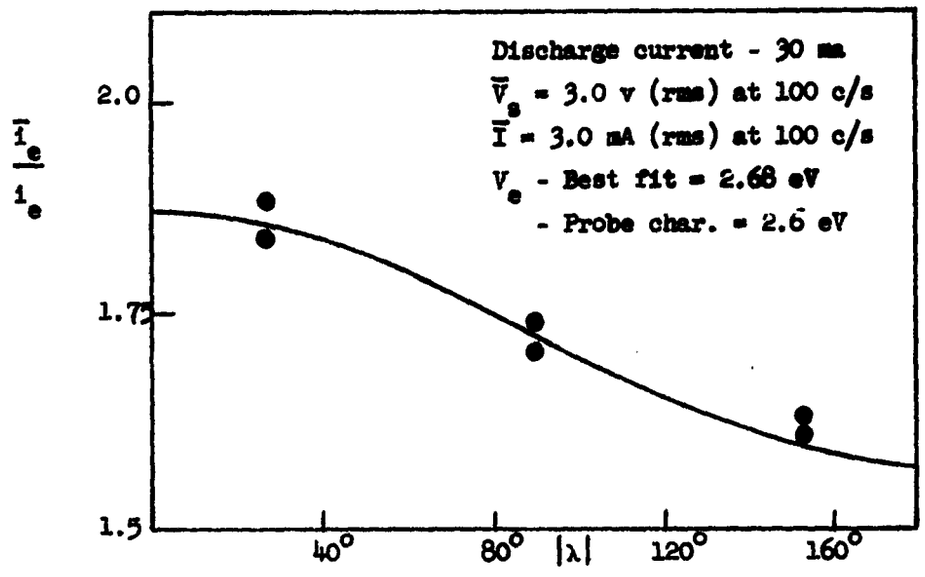

FIG. 5--Probe current increase due to direct and cross-modulation effects.

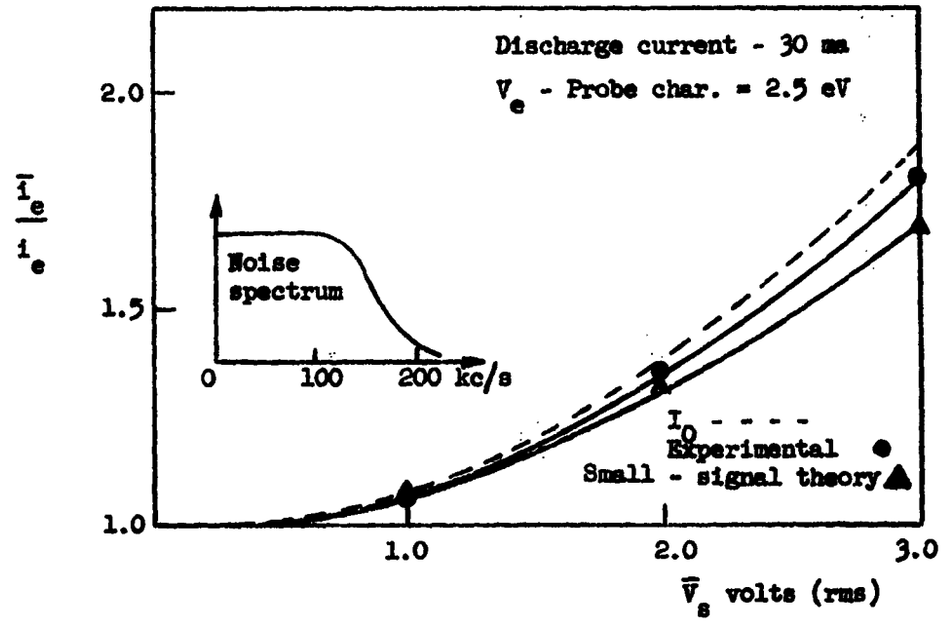

FIG. 6--Probe current increase due to a noise signal in series with the probe.

a wall sheath is not at all certain. One possibility is that the density and potential have a node at the wall as was assumed by Crawford;[13] alternatively, it could be that the density fluctuation has an antinode at the wall, as in an ordinary sound wave. In practice, the boundary condition might lie between these two extremes.

The modes to be expected on a uniform plasma column with the alternative boundary conditions are quite different as are the cut-off frequencies for longitudinal propagation. The cut-off frequencies are given by

$$f_{m,n} = \frac{v_p}{2\pi a} \cdot \alpha_{mn} \quad , \tag{15}$$

where $v_p = (\gamma kT_e/m_i)^{1/2}$ is the phase velocity of a plane wave in the unbounded plasma, and where, for a node at the wall, α_{mn} is the n^{th} root of $J_m'(x) = 0$, while for an antinode at the wall, α_{mn} is the n^{th} root of $J_m(x) = 0$.

For the four modes with lowest frequency in each case, we have

node at wall: $\alpha_{01} = 2.405$, $\alpha_{11} = 3.832$, $\alpha_{21} = 5.135$, $\alpha_{02} = 5.52$.

antinode at wall: $\alpha_{11} = 1.842$, $\alpha_{21} = 3.05$, $\alpha_{01} = 3.832$, $\alpha_{31} = 4.21$.

In the case of the antinode boundary condition a dispersion-free plane wave, $\alpha_{00} = 0$, is possible, i.e., a wave with constant amplitude across the section.

Unfortunately, uncertainty in the appropriate value of γ and the relatively large tolerance in temperature measurement means that the absolute values of the noise peak frequencies do not allow a distinction to be made between the alternative boundary conditions. Further, the ratios of the frequencies of the second, third and fourth peaks to the first are almost identical for the two conditions. They are

node at wall: 1.59, 2.13, 2.29.

antinode at wall: 1.65, 2.05, 2.28.

Two methods of resolving the ambiguity have been pursued. The first has been to try to directly determine the profile of the density fluctuation across the tube from the accompanying light output fluctuations by using a photomultiplier and simple optics arranged to accept light from only a narrow pencil which is traversed across the section. The second approach has been to use tubes for which the frequency ratios with the alternative boundary conditions

are quite different. Two such tubes are shown in Fig. 7. For example, in the case of a rectangular tube with dimensions a,b such that $a/b = k(> 1)$, the cut-off frequencies for a uniform column are given by

$$f_{mn} = \frac{v_p}{2a}\left(n^2 + k^2 m^2\right)^{\frac{1}{2}} = \frac{v_p}{2a} \cdot \beta_{mn} \quad , \qquad (16)$$

where for a node at the wall: $m = 1, 2, 3, \ldots$

$n = 1, 2, 3, \ldots$

the first six modes have $\beta = \sqrt{5},\ 2\sqrt{2},\ \sqrt{13},\ \sqrt{17},\ 2\sqrt{5},\ 5$, while for an antinode at the wall: $m = 0, 1, 2, 3$

$n = 0, 1, 2, 3$,

and the first six values of β are $\beta = 1, 2, \sqrt{5}, 2\sqrt{2}, 3, \sqrt{13}, 4$.

In addition, in the latter case the mode $m = 0$, $n = 0$ is allowed, corresponding to a dispersion-free plane wave with no variation in the cross-section.

The ratio of the lowest frequencies with the alternative boundary conditions is $\sqrt{5} = 2.24$ compared with 1.31 for the circular case, so that the absolute value of the lowest frequency noise peak is more useful in this case. Also, the ratios of the frequencies of succesive peaks to the lowest are quite different with the alternative boundary conditions. They are

node at wall: 1.26, 1.61, 1.84, 2, 2.24

antinode at wall: 2, 2.24, 2.83, 3, 3.61, 4.

Thus, there should be a clear distinction between the mode spectra on the alternative boundary assumptions. Similar considerations apply to the pill-box geometry shown in Fig. 7. These flat tubes have the additional advantage that the light intensity profile is more convenient for study than that of a cylindrical one.

1. Light profile measurements on a cylindrical tube.

Before the rectangular tube became available, near the end of the quarter, light measurements were made using a cylindrical tube of 2.5 cm i.d.

Figure 8 shows the system used to measure the profile of light intensity. The width of the section sampled is controlled by the width of the movable slit (2.5 mm) while the divergence of the section sampled is determined by the ratio of the circular aperture to the focal length of the lens. At first, some difficulty was experienced due to the fact that for different positions

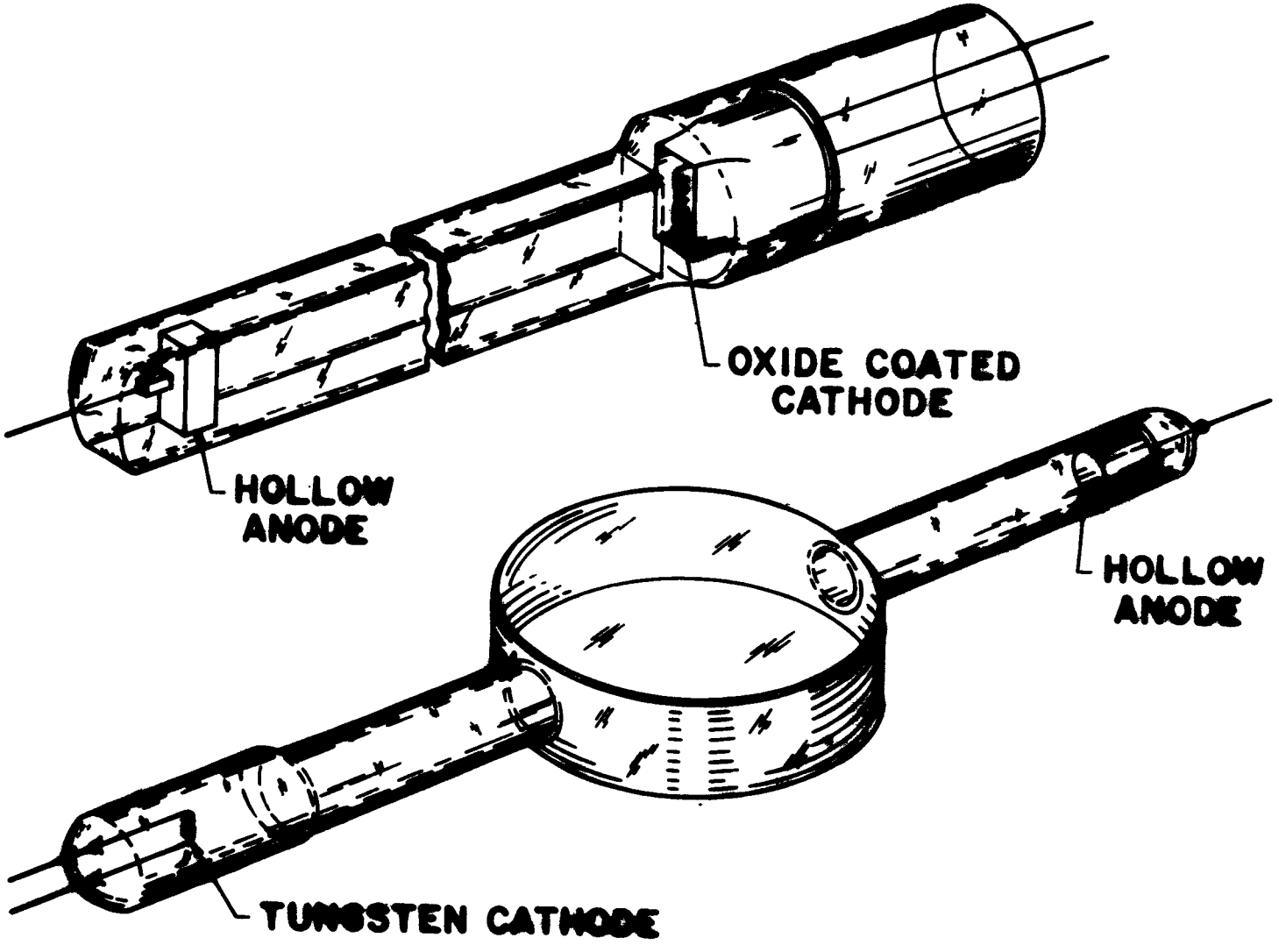

FIG. 7--Experimental discharge tubes.

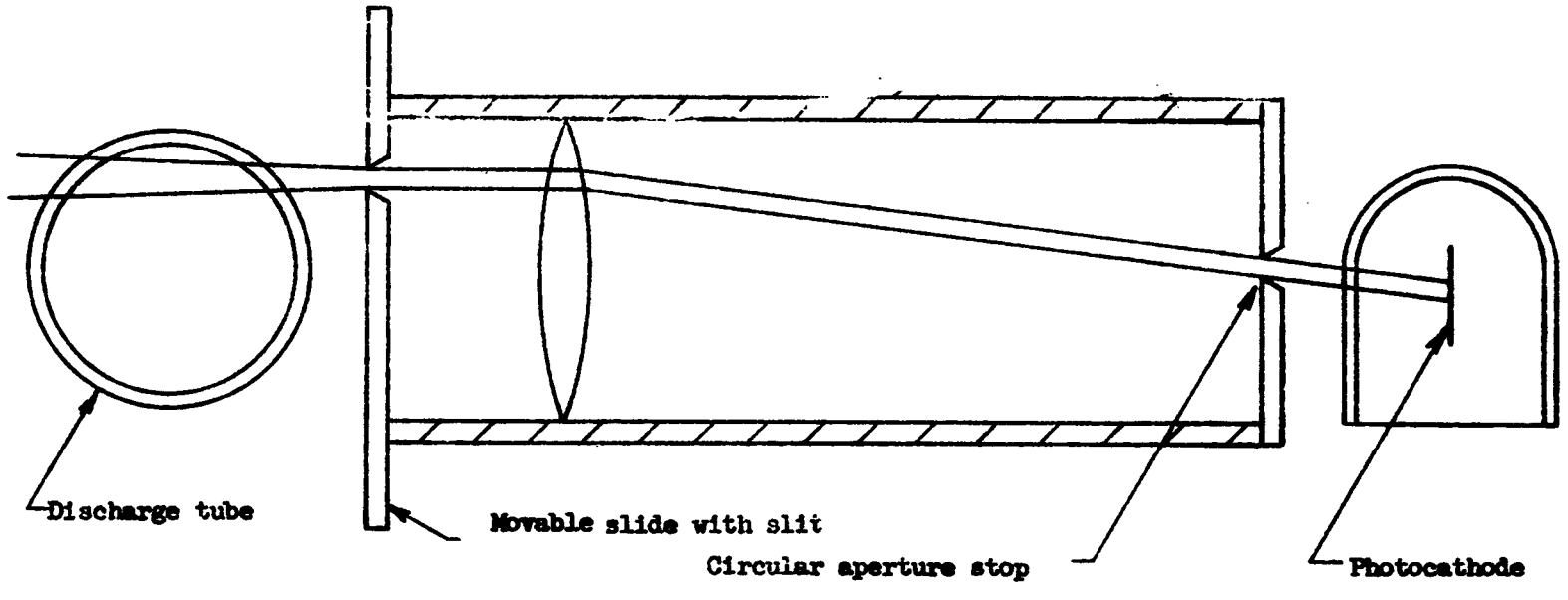

FIG. 8--Optical system.

of the slide, the light tends to fall on different areas of the photocathode. If the sensitivity of the latter varies over its surface, errors are introduced. Careful alignment reduced such errors, though an intrinsically more accurate method would be to keep the slide fixed and move the whole detector bodily at right angles to the tube in an accurately controlled manner.

A measurement taken of the profile of the dc light output at 100 ma tube current is shown in Fig. 9a. Some slight asymmetry of the profile is noticeable and may be due to residual errors due to the reason mentioned above or, possibly due to differing thickness of the glass tube wall or deposits of mercury on the tube wall, though these were avoided as far as possible by gentle local heating of the tube.

Figure 9b shows profiles taken under the same conditions of the ac component of the light output for a superimposed ac current of 30 ma at 1 Kc/s . It is seen that the profiles are virtually identical. Similar measurements were made at frequencies of 100 c/s, 1 kc/s, 10 kc/s, 100 kc/s and 1 Mc/s . There was no great change in the profile, except for 1 Mc/s when it became appreciably more rounded. This suggests that, supposing the light output to be proportional to local electron density, the ac density amplitude is proportional to the dc density at every radius--a not unreasonable result.

In principle, if the intensity profile is measured, it is possible to deduce the intensity of emission as a function of radius.[14] This is a tedious arithmetic transformation and the final answer tends to magnify errors in the experimental curves. Figure 10 shows the result of this transformation on the dc profile. A rather large scatter is evident, and it is clear that considerable refinement of the method is required to give accurate values for the emission as a function of radius. Also plotted is the density to be expected on the basis of the plasma approximation for the low pressure discharge calculated by Tonks and Langmuir.[15]

With no impressed ac current, the photomultiplier output shows a noise spectrum very similar to the noise spectrum of the tube current or voltage with a broad peak around 40 kc/s and a second smaller broad peak around 70 kc/s . The profile of the height of the first noise peak as measured on a spectrum analyzer was next measured. The photomultiplier was located some 14 cm from the constriction where the maximum noise occurred. The result is shown in Fig. 11. It is seen that the profile is very similar to that of the dc light output and

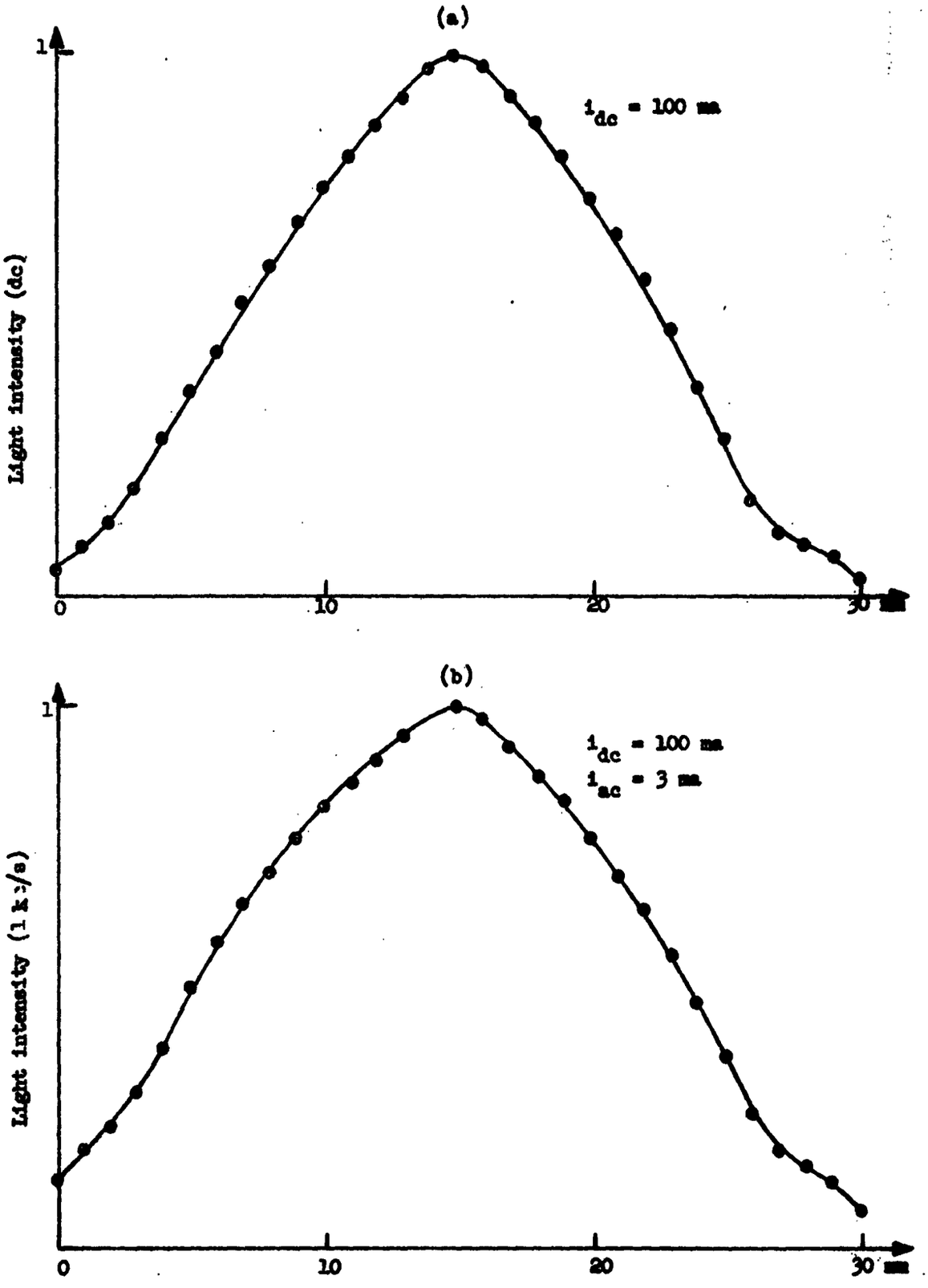

FIG. 9--Light intensity profiles.
(a) Steady signal.
(b) 1 kc/s signal.

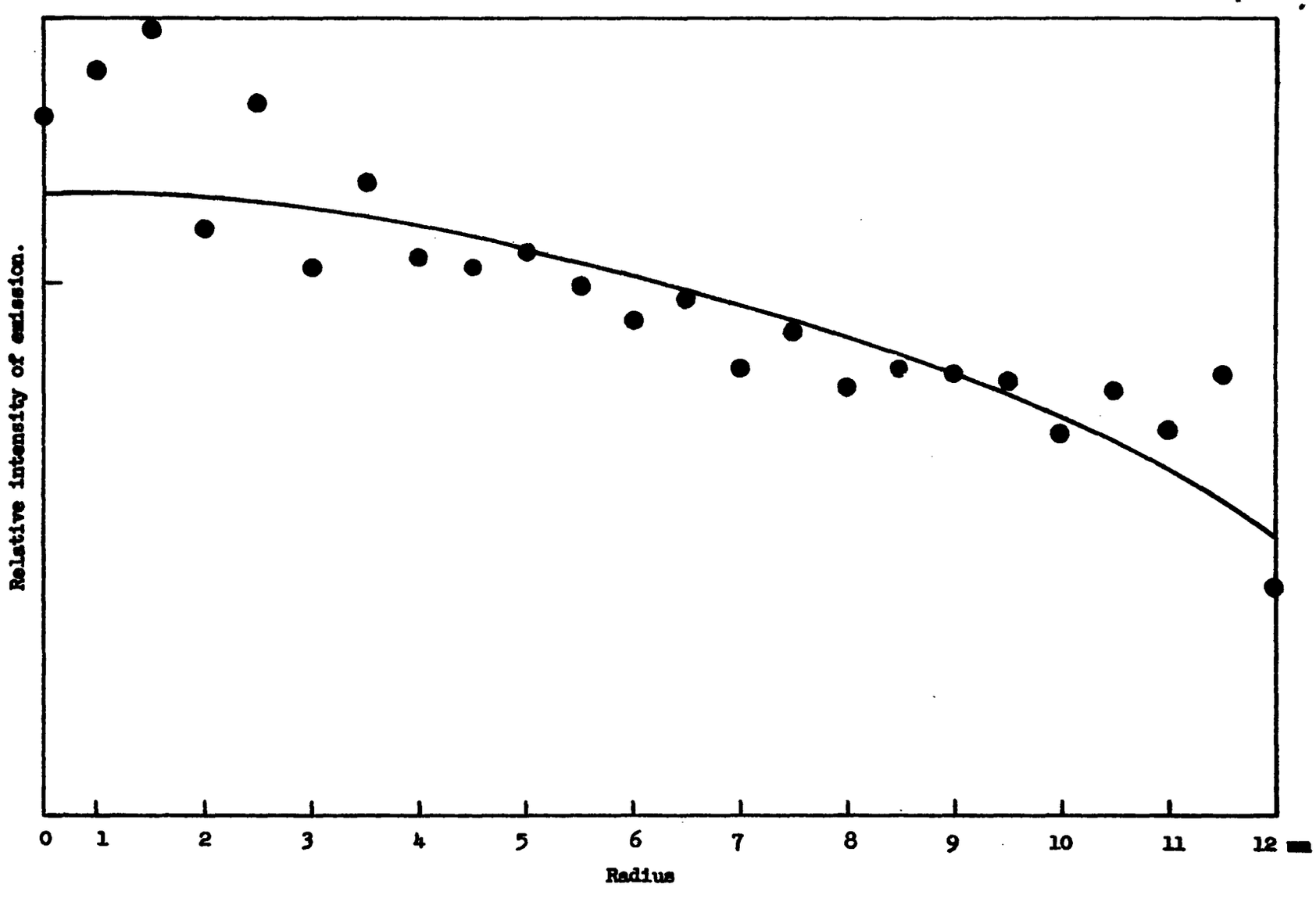

FIG. 10--Light emission as a function of radius.

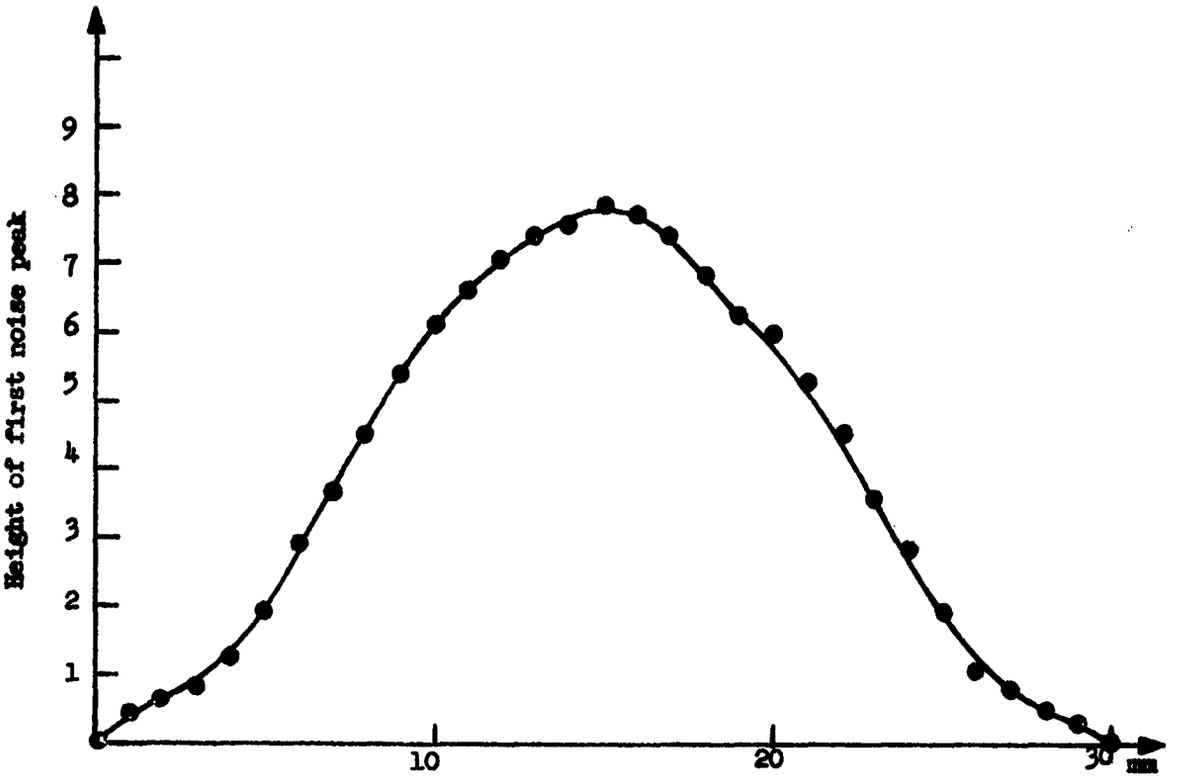

FIG. 11--Profile of light intensity of frequency of first noise peak.

the ac output for impressed currents.

In order to investigate the profile of the noise fluctuation of light intensity further, two identical photomultipliers were used on opposite sides of the discharge. When the two slits were in line with the axis so that the photomultipliers sampled the same central volume, the signals, displayed in Fig. 12a, were very well-correlated. One photomultiplier was now raised and the other lowered until they were accepting light from opposite sides of the discharge, with the result shown in Fig. 12b. It is seen that the signals are still well correlated. Thus these measurements seem to show that the noise fluctuation of the light output is in the same phase across the cross section and that the amplitude approximately follows the same radial variation as the dc light output and hence the steady electron density.

2. Light profile measurements on flat tubes.

The rectangular discharge tube was constructed from three 25 x 3.0 x 1.5 cm lengths of precision tubing. The tube proved to be unusually quiet. This may be due to the way in which the cathode shield was tapered into the rectangular shape of the main tube. It has previously been observed that the noise level is lower on tubes without sudden changes of cross section.

A large number of well-defined peaks were observed in the noise spectrum, extending from ~ 20 - 400 kc/s (Fig. 13). At low currents, less than, say, 50 ma, the peaks were very sharp; at higher currents, say, 100 ma, the peaks were fewer and broader.

Careful measurements were made of the frequencies of these peaks as a function of current in the range 10 to 100 ma. There are some peaks which tune very little with current, others which tune rapidly with current, and in addition, some modes appear only over a limited range of current. A plot of the frequencies of the peaks against current is shown in Fig. 14. Particularly noticeable is a set whose frequencies are quite accurately in the ratios 1:2:3:4. It was established that these are time harmonics of the lowest frequency rather than separate modes.

It was concluded that the narrow, current-dependent peaks observed at the lower currents were not related to the few broad current-independent peaks observed earlier in round tubes.

In some further experiments the effect of lowering the vapor pressure by immersing the cathode end in water at $0^{\circ}C$ was found to be quite drastic. In

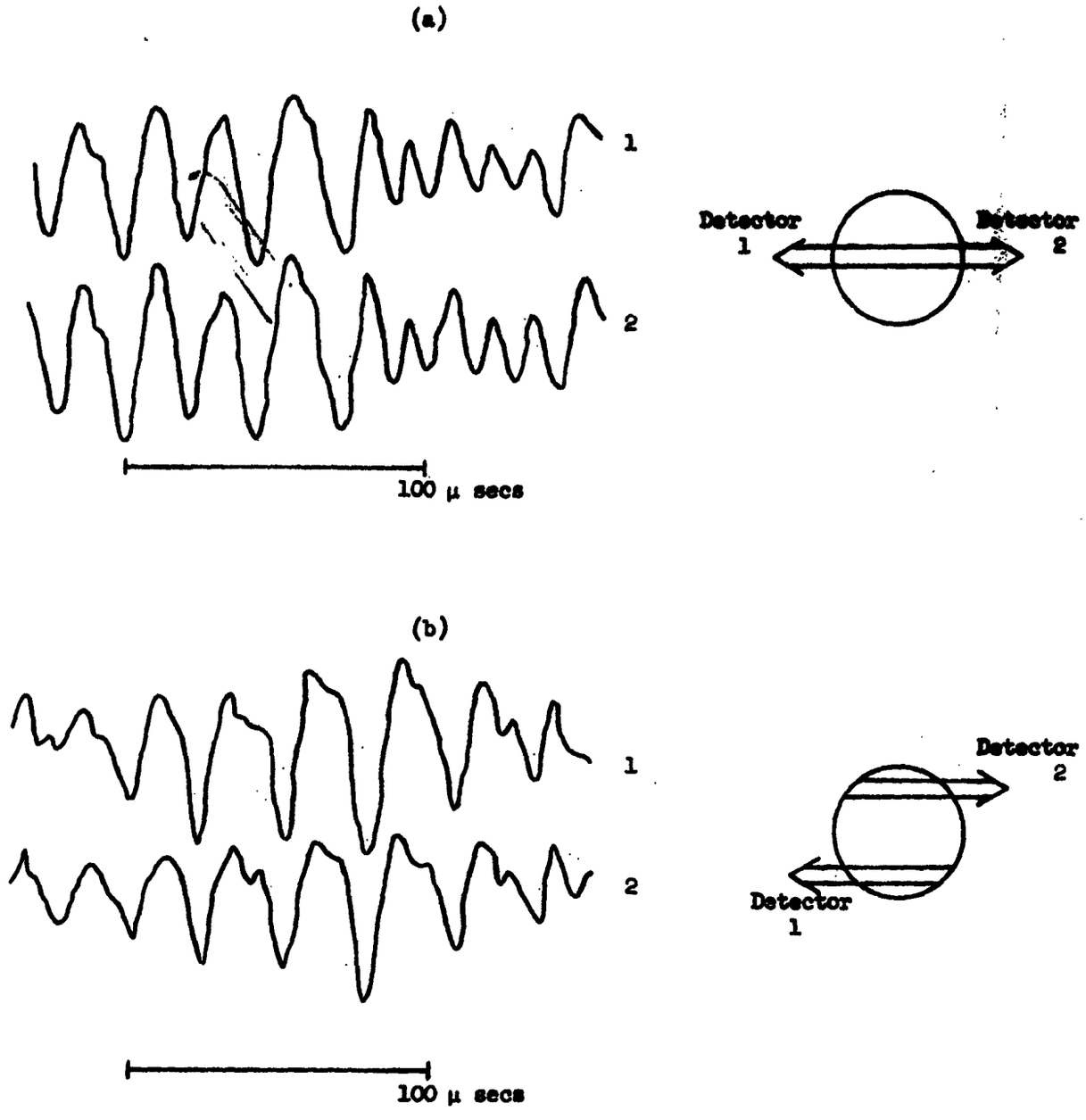

FIG. 12--Correlation of light output fluctuations across tube diameter.

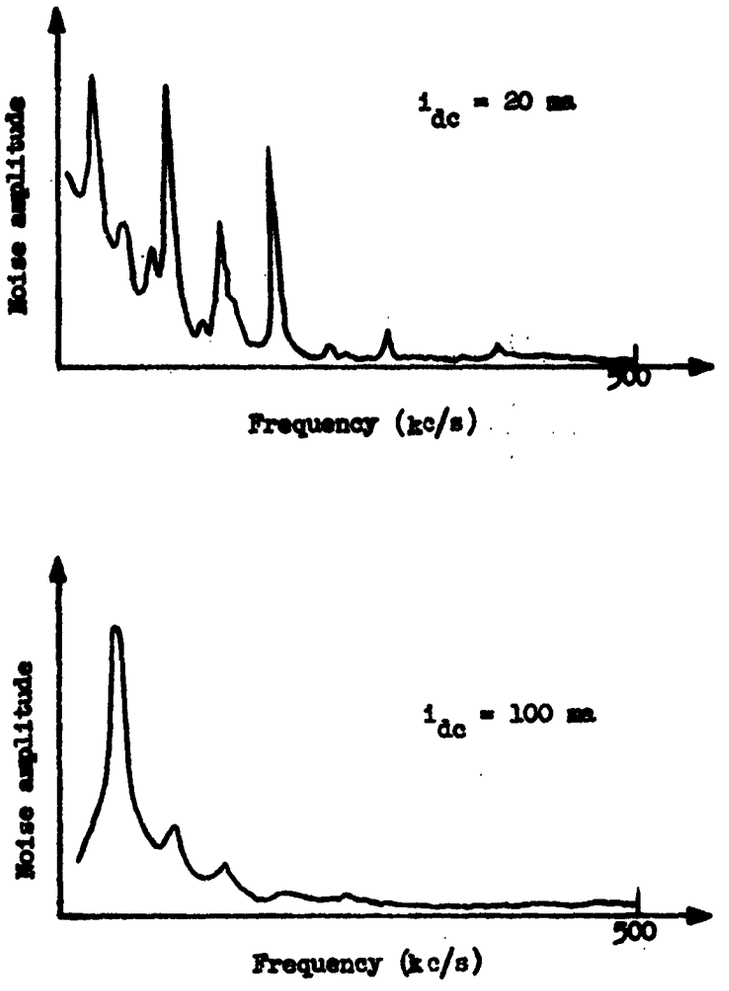

FIG. 13--Noise spectra of rectangular tube.

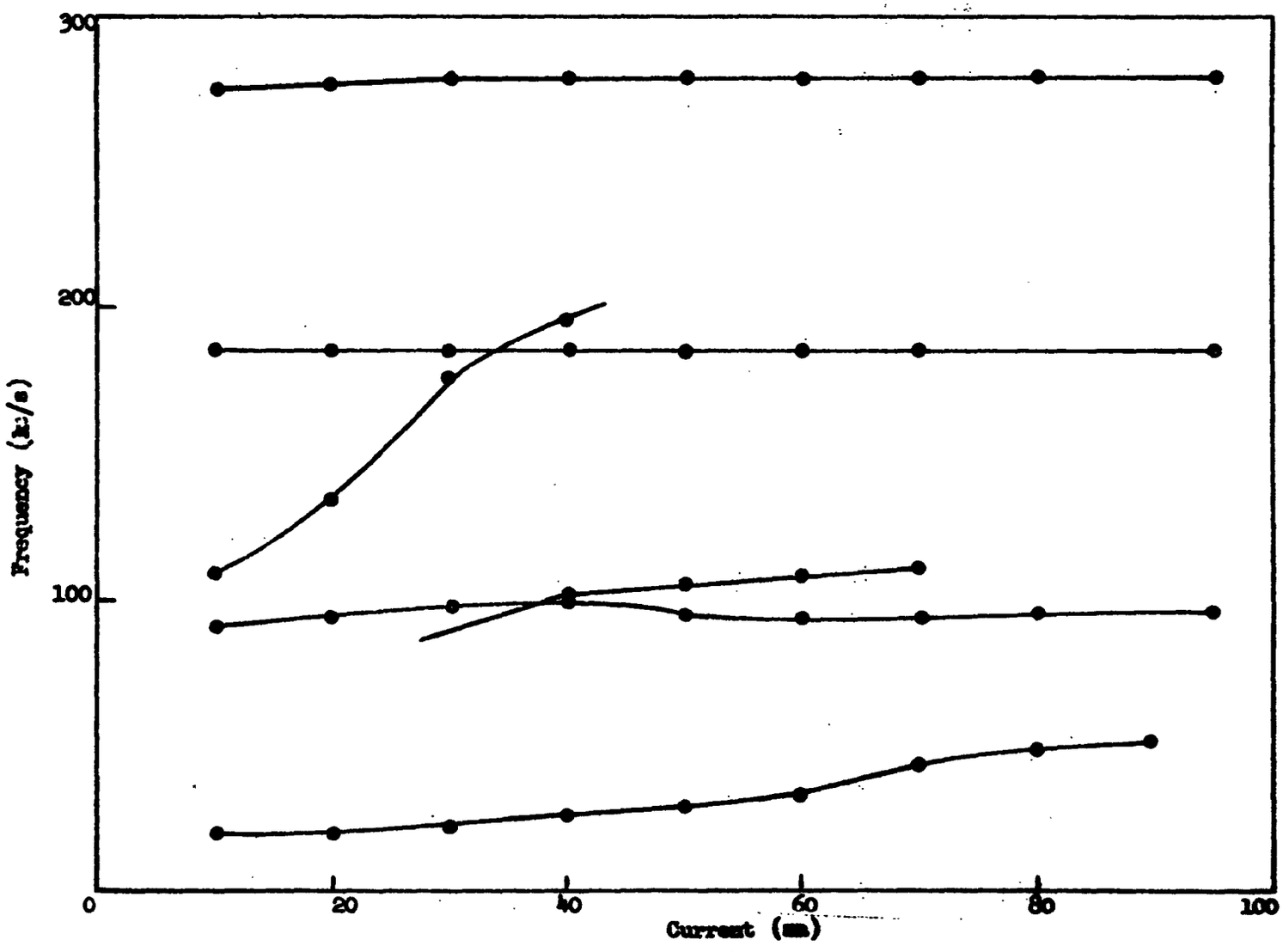

FIG. 14--Frequency of noise peaks as a function of current.

a typical run at 100 ma tube current, at room temperature ($\sim 20^{\circ}C$) broad peaks were observed at 47, 94, 140, 188, 237 and 290 kc/s, which are quite accurately in the ratios 1:2:3:4:5:6. On cooling the tube, these broad peaks virtually disappear, while a few sharp current-dependent peaks appear.

In view of the complexity of the phenomena, there seems little hope of relating these frequencies to the ion wave cut-offs calculated above. It would seem that the peaks corresponding to those observed extensively by Crawford in round tubes are the broad, current-insensitive ones observed at larger currents. Unfortunately, these peaks appear to be all time harmonics of the fundamental one which occurs at 47 kc/s for 100 ma current. Thus it would appear that we are exciting only one mode of the type expected and we cannot deduce anything about the boundary condition from the ratios of peaks, as we had hoped.

However, from the absolute value of the lowest frequency we measure $f_0 = 47$ kc/s at 100 ma tube current so that $f_0(2a) \approx 1.4$ and changes only slowly with current. The theory gives:

for a node at the wall: $f_0(2a) = 1430\ (\gamma T_e)^{1/2}$

for an antinode at the wall: $f_0(2a) = 0\ (\gamma T_e)^{1/2}$.

Thus, on the alternative assumptions we have $(\gamma T_e) \approx 10^4$ and 4.84×10^4, respectively. Since $\gamma \geq 1$ (and very likely $1 \leq \gamma \leq 5/3$), and since the electron temperature under the conditions of the experiment was probably about $30{,}000^{\circ}K$, the antinode assumption is seen to give a better fit. The assumption of a node at the wall does not fit unless the temperature were less than $10{,}000^{\circ}K$, which is considered very unlikely.

Thus, although the results from the spectrum of the rectangular tube are not as positive as had been hoped, they do provide support for the antinode boundary condition.

Preliminary attempts to determine the profile of the noise fluctuation of light output in the rectangular tube were not very promising because the noise level was so low that the shot noise in the photomultiplier was comparable.

The separation of the modes in the pill-box tube was expected to be even greater than in the rectangular tube. The success of the experiment depended on the appearance of the lowest mode for a potential maximum at the wall. A frequency component of roughly the predicted value appeared in certain ranges of current but was somewhat erratic. It was also somewhat dependent on the current. Further tests have been made on this tube which is presently being modified. These results, which will be given in a later report, also seem to incline towards the potential maximum boundary condition at the wall.

C. STRIATIONS

Attempts to observe fixed or moving striations in our mercury-vapor discharges have been reported previously.[3] In other discharges where striations are known to occur, they are generally accompanied by large amplitude low and high frequency noise, so that it is important to know whether or not they will appear under our conditions. Although it did not seem likely that they would do so, detailed observations of such striations in mercury vapor had been reported in one publication.[16]

Some further work was done during the Quarter using improved photomultiplier/amplifier setups. At first, two photomultipliers were used at different positions along the column and correlation between signal and position was looked for, as in our previous experiments and those of Foulds.

Unfortunately, the signal level was found to be so low at points well removed from the cathode and the constriction that the discharge noise/shot noise level was very poor. To improve this two photo-cells followed by video amplifiers were used in place of the photomultipliers. By arranging for the photo-cells to accept much more light from the discharge than is permitted with the photomultipliers, the discharge noise signal/shot noise can be significantly improved since the "signal" is proportional to the light intensity while the shot noise is proportional to the square root of the steady light level. Using the phototubes, a series of double trace oscilloscope shots were taken starting with both photo-tubes looking at the same point in the discharge and then as one was moved to various positions along the tube. With both photo-cells looking at the same point in the discharge, the correlation was excellent. As one tube was moved along the tube, the correlation gradually decreased. As a check, the outputs from the two photo-cells were applied to the X and Y plates of an oscilloscope. When the photo-cells were looking at the same point, the trace appeared as a straight line. As one photo-cell was moved along the tube, the straight line gradually degenerated into a diffuse spot signifying no correlation between the signals.

Similar measurements were taken using two strip-lines instead of two phototubes to see if there was any correlation or evidence of moving striations in terms of the number density fluctuation. Results were similar to those obtained with the light output.

An account of our work on striations and a discussion of their mechanisms and probability of appearing in low-pressure mercury-vapor discharges are given in Microwave Laboratory Report No. 962.[17]

D. IMPEDANCE

To complement the theoretical work described in Section III.B, measurements of plasma impedance have been made in a tube containing a movable anode. It was hoped that it might then be possible to separate the impedances of the positive column and the electrode regions. It was found, however, that the commercial bridge used could only operate at low signal levels which were difficult to detect in the presence of the discharge noise. More recently, consideration has been given to alternative experimental methods and schemes involving direct display of the impedance locus on an oscilloscope. These will be reported at a future date.

E. DOUBLE SHEATHS AT TUBE CONSTRICTIONS

It has been remarked frequently in the course of this work that tubes having a constriction in the column are usually considerably more noisy than those without, and that noise is generated at, or near to this constriction. Since the plasma has different number densities and electron temperatures in the two sections a double-sheath might be expected to form at the constriction to prevent a net current flowing from the smaller to the larger section.

Since double-sheaths near cathodes seem to have high and low-frequency noise associated with them, it seems likely that these constriction sheaths will be accompanied by similar phenomena. Little appears to be known about them, other than that they exist, so a special discharge tube has been constructed to study them. This is shown in Fig. 15. The moving prove may be traversed from anode to cathode. For part of the work carried out under another contract an instrument was constructed which can be used to give the second differential of the probe current/voltage characteristic. This can be interpreted to give the electron velocity distribution.[18] Preliminary measurements indicate that the sheath occurs in a narrow region < 2 mm thick, close to the constriction. The voltage drop across the sheath can be predicted on the basis of a simple theory which is presently being developed, and for the experimental tube is 5-10 V .

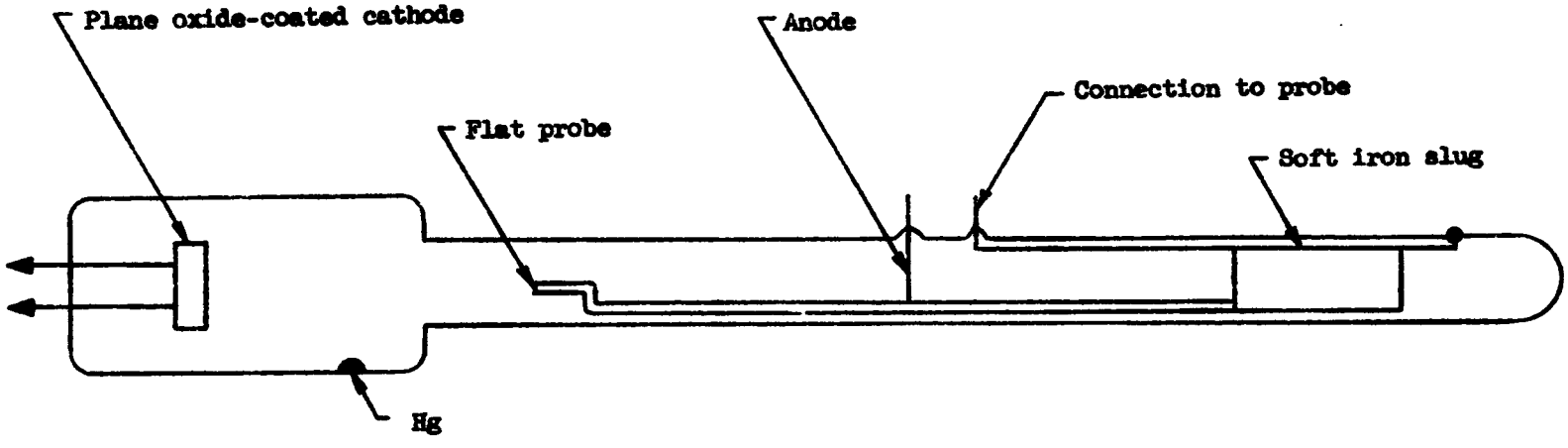

FIG. 15--Experimental discharge tube.

V. DISCUSSION AND FUTURE PROGRAM

In the coming quarter it is hoped that our theory of plasma impedance will be extended to include secondary effects and that we can improve the agreement with experimental results. The theory of dipole resonances is to be checked in the plane geometry already available in the pill-box tube of Fig. 7. We also hope to check some tentative theory proposed for the case of dipole resonance in a cylindrical discharge tube lying in an axial magnetic field.

Further work will be carried out on ion waves to elucidate their boundary conditions, and to this end some propagation experiments are envisaged, together with examination of resonances in a modified design of the pill-box tube.

The light output studies will be continued, with more attention paid to the individual spectral lines. Study of these, it is hoped, will help to clarify the maintaining mechanism of the discharge, which in turn determines whether or not oscillations are an intrinsic factor in its survival or not.

LIST OF REFERENCES

1. Quarterly Status Report No. 11 for Contract AT(04-3)-326-1, Microwave Laboratory Report No. 959, Stanford University (October 1962).
2. Quarterly Status Report No. 8 for Contract AT(04-3)-326-1, Microwave Laboratory Report No. 919, Stanford University (May 1962).
3. Quarterly Status Report No. 7 for Contract AT(04-3)-326-1, Microwave Laboratory Report No. 965, Stanford University (October 1961).
4. F. W. Crawford, G. S. Kino, S. A. Self, and J. Spalter, Microwave Laboratory Report No. 961, Stanford University (October 1962).
5. F. W. Crawford and G. S. Kino, Microwave Laboratory Report No. 974, Stanford University (October 1962).
6. A. M. Messaien and P. E. Vandenplas, J. Nuc. Energy Pt. C, 4, 267 (1962).
7. F. W. Crawford, Microwave Laboratory Report No. 979, Stanford University (November 1962).
8. F. W. Crawford and J. D. Lawson, J. Nuc. Energy Pt. C, 3, 179 (1961).
9. F. W. Crawford, J. Appl. Phys. 33, 20 (1962).
10. R. M. Howe, J. Appl. Phys. 24, 881 (1953).
11. A. Garscadden and K. G. Emeleus, Proc. Phys. Soc. 79, 535 (1962).
12. F. W. Crawford, Microwave Laboratory Report No. 980, Stanford University (November 1962).
13. F. W. Crawford, Phys. Rev. Letters 6, 663 (1961).
14. W. J. Pearce, in "Proceedings of Conference on Extremely High Temperatures," Edited by H. Fischer and L. L. Mansur, Wiley (1958).
15. L. Tonks and I. Langmuir, Phys. 34, 876 (1929).
16. K. W. H. Foulds, J. Elect. and Cont. 2, 270 (1956).
17. F. W. Crawford and H. R. Pagels, Microwave Laboratory Report No. 962, Stanford University (October 1962).
18. F. W. Crawford, Microwave Laboratory Report No. 872, Stanford University (December 1961).

DISTRIBUTION LIST

CONTRACT AT(04-3)-326-1

ASTIA (10)
Arlington Hall Station
Arlington 12, Virginia

A. E. Ruark, Chief (2)
Controlled Thermonuclear Branch
Division of Research
U. S. Atomic Energy Commission
Washington 25, D. C.

C. Van Atta (2)
University of California
Lawrence Radiation Laboratory
P. O. Box 808
Livermore, California

J. L. Tuck (2)
Los Alamos Scientific Laboratory
P. O. Box 1663
Los Alamos, New Mexico

A. H. Snell (2)
Oak Ridge National Laboratory
P. O. Box Y
Oak Ridge, Tennessee

M. B. Gottlieb (2)
Project Matterhorn
Princeton University
P. O. Box 451
Princeton, New Jersey

S. Chandrasekhar
Yerkes Observatory
Williams Bay, Wisconsin

W. A. Fowler
W. K. Kellogg Radiation Laboratory
California Institute of Technology
Pasadena, California

W. R. Faust
Radiation Division, Bldg. 65
Naval Research Laboratory
Washington 25, D. C.

H. S. Robertson
Department of Physics
University of Miami
Coral Gables 46, Florida

R. Hines
Northwestern University
Department of Physics
Evanston, Illinois

S. C. Brown
Massachusetts Institute of Technology
Research Laboratory of Electronics
Cambridge 39, Massachusetts

W. H. Brummett, Jr.
U. S. Atomic Energy Commission
2111 Bancroft Way
Berkeley 4, California

W. H. Bostick
Stevens Institute of Technology
Department of Physics
Hoboken, New Jersey

Paul D. Coleman
Department of Electrical Engineering
University of Illinois
Urbana, Illinois

E. G. Harris
University of Tennessee
Department of Physics and Astronomy
Knoxville, Tennessee

R. Hughley
U. S. Atomic Energy Commission
San Francisco Operations Office
518 17th Street
Oakland 12, California

W. M. Gottschalk
University of Delaware
Newark, Delaware

S. K. Allison
The Enrico Fermi Institute for
Nuclear Studies
The University of Chicago
Illinois

R. E. Fox
Physics Department
Westinghouse Research Laboratories
Beulah Road, Churchill Boro
Pittsburgh 35, Pennsylvania

W. P. Allis
Research Laboratories of Electronics
Massachusetts Institute of Technology
Cambridge 39, Massachusetts

David Beard
Department of Physics
University of California
Davis, California

J. W. Butler
Argonne National Laboratories
P. O. Box 299
Lemont, Illinois

L. H. Fisher
Department of Physics
New York University
University Heights
New York 53, New York

AEC Computing and Applied Math Center
New York University
9 Washington Place
New York 3, New York
Attn: Director

H. Hurwitz, Jr.
Nucleonics and Radiation Division
General Electric Company
Research Laboratory
P. O. Box 1088
Schenectady, New York

P. E. C. Corporation
1001 Mapleton Avenue
Boulder, Colorado

Donald Kerr
Johns Hopkins University
Department of Physics
Baltimore 18, Maryland

J. C. Clarke
U. S. Atomic Energy Commission
New York Operations Office
70 Columbus Avenue
New York 23, New York

K. A. Dunbar
U S. Atomic Energy Commission
Chicago Operations Office
P. O. Box 59
Lemont, Illinois

Samuel Koslov
Stevens Institute of Technology
Department of Physics
Hoboken, New Jersey

S. R. Sapirie, Manager
U. S. Atomic Energy Commission
Oak Ridge Operations Office
P. O. Box E
Oak Ridge, Tennessee

E. C. Shute, Manager
U. S. Atomic Energy Commission
San Francisco Operations Office
2111 Bancroft Way
Berkeley, California

L. Spitzer, Jr.
Project Matterhorn
James Forrestal Research Center
P. O. Box 451
Princeton, New Jersey

D. W. Kerst
General Dynamics Corporation
General Atomic Division
P. O. Box 608
San Diego 12, California

A. J. Hatch
Argonne National Laboratories
P. O. Box 299
Lemont, Illinois

John W. Flowers
University of Florida
Dept. of Physics and Nuclear Engineering
Gainesville, Florida

Cornell University
School of Electrical Engineering
Ithaca, New York
Attention: Prof. G. C. Dalman

William I. Lindor
Hughes Research Laboratories
P. O. Box 338
Malibu, California

H. Wilhelmsson
Research Laboratory of Electronics
Chalmers Institute of Technology
Gibraltargatan 5 G
Gothenburg, Sweden

Technical Information Service Extension
Atomic Energy Commission
P. O. Box 62
Oak Ridge, Tennessee

Institute for Defense Analysis
Research and Engineering Support Division
1825 Connecticut Avenue, N. W.
Washington 9, D. C.
Attn: Technical Information Office

Dr. John M. Teem
Electro-Optical Systems, Inc.
125 N. Vinedo Street
Pasadena, California

Matthew Allen
Microwave Associates Inc.
Burlington, Massachusetts

Mauro Di Domenico
Bell Telephone Laboratories
Murray Hill, New Jersey

B. Meltzer
Department of Electrical Eng.
The University
Mayfield Road
Edinburgh 9, Scotland

CERN
Service d'Information Scientifique
Geneva 23, Switzerland
Attn: L. Goldschmit-Clermont

J. F. Kane
Kane Engineering Laboratories
845 Commercial Street
Palo Alto, California

William B. Pardo
Department of Physics
University of Miami
Coral Gables 46, Florida

Electron Tube and Microwave Laboratory
California Institute of Technology
Pasadena, California
Attn: D. E. Dow

George Schmidt
Department of Physics
Stevens Institute of Technology
Hoboken, New Jersey

Bomac Laboratories, Inc.
Research and Development
Salem Road
Beverly, Massachusetts
Attn: Arthur McCoubrey

Behram Kursunoglu
Department of Physics
University of Miami
Coral Gables 46, Florida

Robert Betchov
Physical Research Laboratory
Aerospace Corporation
2400 East El Segundo Boulevard
El Segundo, California

Prof. P. Clarricoats
Department of Electrical Eng.
University of Sheffield
St. Georges Sq.
Mappin St.
Sheffield 1, England

Ervin J. Nalos
Boeing
P. O. Box 3707
Seattle 24, Washington